Atmosphere **2014**, *5*, 435-453; doi:10.3390/atmos5020435

OPEN ACCESS

atmosphere

ISSN 2073-4433

www.mdpi.com/journal/atmosphere

Article

Characterization of PM_{10} and $PM_{2.5}$ and Their Metals Content in Different Typologies of Sites in South-Eastern Italy

Daniele Contini [1,*], Daniela Cesari [1], Antonio Donateo [1], Daniela Chirizzi [1] and Franco Belosi [2]

[1] Istituto di Scienze dell'Atmosfera e del Clima (ISAC), CNR, Str. Prv. Lecce-Monteroni km 1.2, 73100 Lecce, Italy; E-Mails: d.cesari@isac.cnr.it (D.C.); a.donateo@isac.cnr.it (A.D.); d.chirizzi@le.isac.cnr.it (D.C.)

[2] Istituto di Scienze dell'Atmosfera e del Clima (ISAC), CNR, Via Gobetti 101, 40129 Bologna, Italy; E-Mail: f.belosi@isac.cnr.it

* Author to whom correspondence should be addressed; E-Mail: d.contini@isac.cnr.it; Tel.: +39-0832-298919; Fax: +32-0832-298716.

Received: 20 March 2014; in revised form: 6 May 2014 / Accepted: 15 May 2014 / Published: 16 June 2014

Abstract: Samples of PM_{10} and $PM_{2.5}$ were collected discontinuously between 2003 and 2010 at fifteen monitoring sites (urban, background, industrial) in the south-eastern part of Italy using a mobile laboratory. In total, 483 PM_{10} and 154 $PM_{2.5}$ samples were collected and chemically analyzed for the determination of metal content. Data were used to investigate concentration differences among the typologies of sites, the seasonal patterns, and the influence of advection of Saharan dust (SD). PM_{10} and $PM_{2.5}$ average concentrations increase from background to industrial and urban sites but the ratio $PM_{2.5}/PM_{10}$ is significantly lower (0.61 ± 0.10) in background sites. The average metals concentrations in PM_{10} and in $PM_{2.5}$ do not show a clear dependence on site typology apart an increase in crustal elements in background sites and an increase in the enrichment factors of Ni and of Cr in PM_{10} in industrial sites. Urban sites show a statistically significant increase of PM_{10} average concentration during the cold seasons (autumn and winter), likely associated with the anthropogenic urban emissions, instead, the background sites show a decrease in concentrations during the cold seasons. This could be due to more frequent cases of SD observed in spring and summer periods that mainly influence background sites. The seasonal difference on the average concentration for industrial sites is not statistically significant. The SD cases influence both PM_{10} and $PM_{2.5}$ concentrations but their effect is significantly larger on PM_{10}. Over the studied area, the effect is relatively limited on long-term average PM_{10} (estimated increase of 3.2%) and $PM_{2.5}$ (estimated increase of 1.5%) concentrations but it

is significant on daily concentrations. It is estimated an increase of 22% of the probability to overcome the air quality standard daily threshold for PM_{10}.

Keywords: $PM_{2.5}$; PM_{10}; metals concentrations; enrichment factors; Saharan dust events

1. Introduction

The term particulate matter (PM) is used to describe solid or liquid particles that are airborne and transported and dispersed in atmosphere. Particles vary in number, size, shape, surface area, chemical composition, and solubility. PM originates from a variety of natural or anthropogenic sources and possesses a range of morphological, physical, chemical, and thermodynamic properties [1]. The current interest in PM is mainly due to its effect on human health [2–4] and its potential role in climate change [5]. Epidemiological studies show different associations between adverse health effects and particles with aerodynamic diameters lower than 2.5 μm ($PM_{2.5}$) and lower than 10 μm (PM_{10}) [6,7].

The sources of PM_{10} and $PM_{2.5}$ include a wide range of natural phenomena and human activities. Coarse (super-micrometric) particles mainly originate from sea salt, soil dust resuspension, construction/demolition activities, non-exhaust vehicle emissions, and industrial fugitives, whereas fine (sub-micrometric) particles are mainly produced by combustion processes, forest fires and transformation of gaseous species. National and International directives and legislations require lower and lower ambient near-surface PM concentrations. The European Union fixed a 24-h PM_{10} mass concentration threshold of 50 $\mu g/m^3$, allowing for less than 35 yearly excesses (EU-Directive 2008/50/CE). The threshold for the annual mean of PM_{10} is 40 $\mu g/m^3$. In addition to the existing threshold values for PM_{10} the EU-Directive has introduced an annual threshold for $PM_{2.5}$ that will be 25 $\mu g/m^3$ from 2015 onwards and 20 $\mu g/m^3$ from 2020. The limits on $PM_{2.5}$ are currently under discussion and subjected to a possible revision, however; it appears that there is an intention In Europe to set a threshold for $PM_{2.5}$ in a similar way to that already existing in USA legislation.

The fixed monitoring networks in the south-eastern part of Italy is mainly based on PM_{10} measurements and is concentrated on urban areas so that there is a general lack of data in this part of Italy, especially regarding $PM_{2.5}$ concentrations and compositions in background sites. As a consequence, this area was not included in the review of PM at kerbside, urban, rural, and background sites in Europe [8].

The Mediterranean area is a region subject to fluxes of anthropogenic and natural particles from Northern Europe and from the African continent (mainly Sahara-Sahel desert) as a consequence of its geographic location. In Mallone *et al.* [9] it was found that the increase of PM concentration associated with advection of African dust in Central Italy had observable health effects and the same was observed in other countries of the Mediterranean Basin [10,11]. The European air quality Directive (2008/50/EC) provides Member States with the possibility to subtract the contribution of natural air pollution sources (like SD events) before comparing atmospheric concentrations with air quality standards. A methodology has been developed to individuate SD events from standard monitoring network measurements [12] to investigate the SD contribution in several European areas. However, information regarding the south-eastern part of the Mediterranean basin are still scarce [13,14] even if

dust advection follows a preferential eastwards transport pattern giving a higher dust contribution in the Eastern Mediterranean basin and increasing from North to South [14]. Further, the meteorology of the area also favors the aging of pollutants, thus inducing high levels of aerosols and photo-oxidant gases [15,16]. The analysis of sites of different typology could help in discriminating local sources from long-range transport.

In this work the long-term concentrations and compositions (trace metals concentrations) of atmospheric aerosol (PM_{10} and $PM_{2.5}$) were investigated in the Salentum Peninsula (Apulia Region, south-eastern part of Italy) using a mobile laboratory. Aerosol samples were collected discontinuously from 2003 to 2010 at fifteen different monitoring sites. The sampling sites have different characteristics and they are classified as urban background sites, urban background near industrial sites and urban sites. The aims of this study are to evaluate similarities and differences of the different typologies of sites, to characterize seasonal differences, and to characterize the impact of Saharan dust advection to observed concentrations and air quality.

2. Instruments and Methods

Measurements were taken in the Salentum peninsula, located in the south-eastern part of Italy (Apulia region), with special focus on the area of the province of Lecce (Figure 1). This area covers a surface of 2759 km^2 with approximately 814,500 inhabitants. It presents a mostly flat orography with a small hills karst area in SW zone, along the central axis of the peninsula (Figure 1). The peninsula has a maximum height of 209 m (a.s.l.) and a central depression zone located north of the main town of Lecce (89,900 inhabitants), which extends down to the cities of Maglie (14,800 inhabitants) and Galatina (27,100 inhabitants). The main pollution sources are associated with urban activities and small (local) industrial emissions. However, the peninsula could be subjected to transport of pollutants from two large industrial settlements located in Taranto and Brindisi at approximately 80 km·W and 37 km·NNW, respectively, from the town of Lecce.

The peninsula has a meteorology characterized by two prevalent wind directions: NNW and SSE with the most intense winds associated with the NNW direction. There is often a convergence of breeze from the Adriatic Sea and from the Ionian Sea with relatively low wind in the central part of the peninsula creating conditions unfavorable to the dispersion of atmospheric pollutants. The typical yearly precipitations are approximately 600 mm, concentrated mostly (about 70% of the yearly precipitations) in the period between October and March, leading to a relatively dry and hot period in the summer season.

In this work, a mobile laboratory was employed to gather information on atmospheric aerosol concentrations (PM_{10} and $PM_{2.5}$) and on aerosol metal content in different typologies of sites: urban background sites (in the following background), urban background sites located near industrial complexes (in the following industrial), and urban sites (in the following urban). PM_{10} and $PM_{2.5}$ samples were collected in measurement campaigns (2–3 weeks long) in different periods between 2003 and 2010. In total, 15 different sites were investigated and, in some sites, multiple measurement campaigns were performed. In Figure 1, the positions of the different sites are shown, together with their classification in the three mentioned typologies. Globally, 483 samples of PM_{10} and 154 samples of $PM_{2.5}$ have been collected and analyzed. The measurement periods were: Lecce background (July

2002, February–March 2003, May 2003, July 2003, December 2003, February–April 2004, May–June 2005; January–November 2007, January 2008); Seclì (July 2006); Galatone (May 2005); Trepuzzi (October–November 2007); Leverano (May 2008); Nardò background (January 2009); Maglie industrial (October 2003, January 2004; November 2004; November 2006; November 2007; September 2008); Collemeto (October 2005); Cutrofiano (April 2004, Junuary–July 2006, November 2008); Tricase (December 2005); Copertino (March 2006); Nardò urban (October–November 2006); Maglie urban (January–February 2007); Lequile (March 2008); Lecce urban (March–April 2010).

Figure 1. Map showing the positions of the measurement sites. The colors indicate the typology of the site (green = background; yellow = industrial; red = urban). The small inset in green reports the orography of the area.

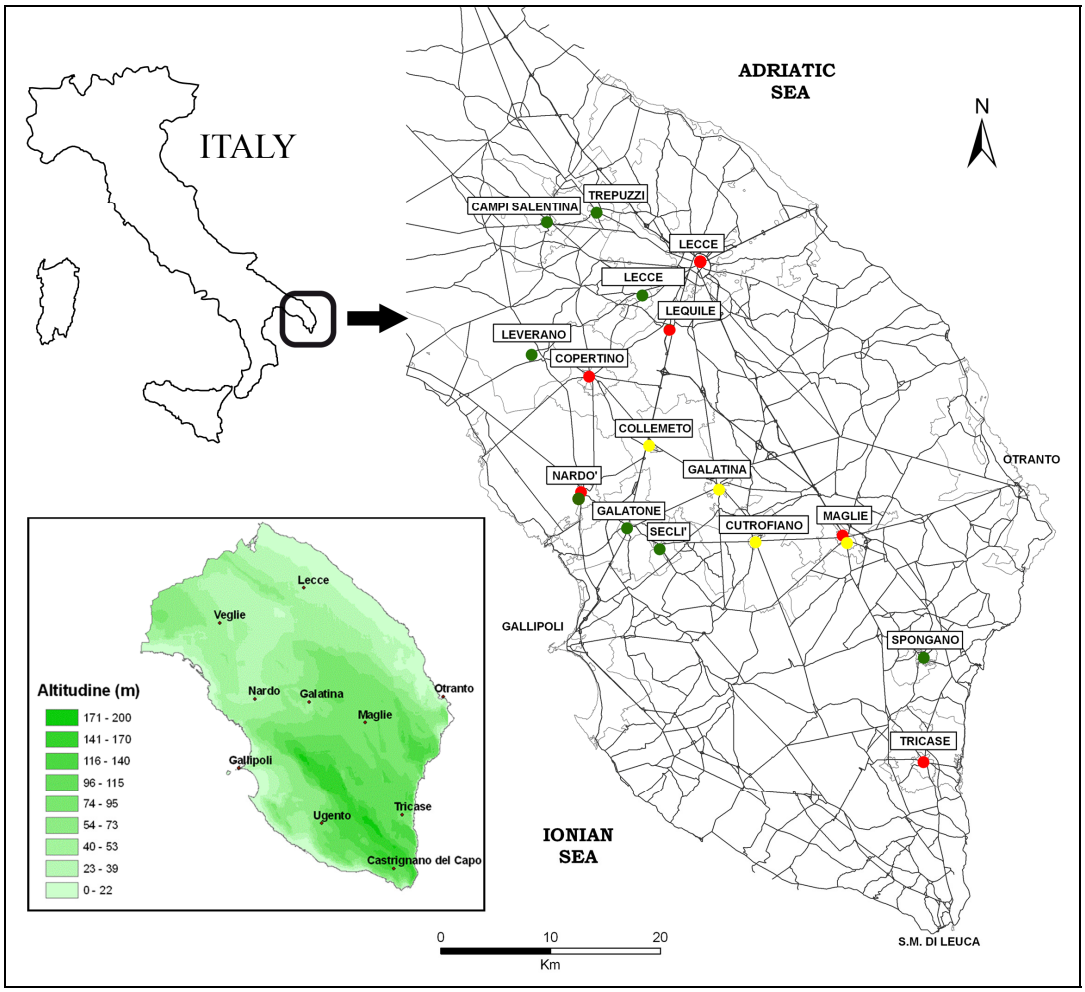

The aerosol samples were collected on substrates (47 mm in diameter), mainly using quartz filters (Quartz-Microfiber Discs, Sartorius) for 24 h (starting from midnight) at low volume (2.3 m^3/h). PM_{10} samples were collected using a sequential automatic sampler (Thermo-Andersen FEQ95SEQ) and $PM_{2.5}$ samples were collected using manual samplers (Tecora Delta and Tecora Bravo H-Plus). During the first few measurement campaigns, cellulose nitrate and polycarbonate filters were also used for aerosol collection but no significant improvements were observed in terms of detection thresholds; therefore, quartz filters were used afterwards. Flow-rate calibrations of the aerosol samplers were performed for each measurement campaign using a rotameter (until 2007) and an electronic calibrator

(Tecora DeltaCal, starting from 2007). The collected samples were stored at 4 °C before gravimetric and chemical analyses. The samples were collected in series (typically 2–3 weeks long) and gravimetric and chemical analyses were performed separately on each series. Gravimetric detection of the mass of collected particles was done using a microbalance (Sartorious, ±1 μg sensitivity), as average of three independent measurements. All filters were weighted before and after sampling, after conditioning for 48 h at the same temperature and humidity of the microbalance, in an air conditioned room, in order to reduce the interference of relative humidity. Field blank filters were used to correct the eventual systematic errors and to evaluate measurement uncertainty through the statistical analysis of blanks [17,18]. Generally, 3–4 field blanks were taken for each measurement campaign. The LOD was determined as three standard deviations of blank filters mass and converted in concentration using the nominal sampling volume of 55.2 m^3. The value obtained (average over all the series) is 2.5 $\mu g/m^3$. The final random uncertainty on measured PM_{10} and $PM_{2.5}$ concentrations was evaluated by combining the uncertainty on the weighting (2 standard deviations of blank filters) and the uncertainty on the sampled volume (2%). Results gave a typical uncertainty between 1 and 3 $\mu g/m^3$.

The quartz filters sampled were chemically analyzed for the determination of concentrations of some metals. Acid digestion of the sampled filters was made with a microwave oven using 1 mL of H_2O_2, 2 mL of HF and 4 mL of HNO_3. After cooling, 0.7 g of H_3BO_3 was added to permit the complexation of fluoride ions and to dissolve the formed fluoride salts. After a final digestion, the solution was analyzed via Graphite Furnace Atomic Absorption Spectroscopy (GF-AAS) for determining 8 elements (Ni, Cu, V, Mn, As, Pb, Cr, Sb, and Cd) and by Inductively Coupled Plasma Atomic Emission Spectroscopy (ICP-AES) for 4 elements (Fe, Al, Zn, and Ti). The chemical analyses were performed partly at the Materials Science Department of the University of Salento and partly at the Multilab Laboratory in Lecce. Results of the analytical determinations were obtained with the removal of the average level present in the blank samples for each chemical species. For each sample, the calculated concentration for a specific species was quantified if it was larger than the standard deviation σ_B of the blank filters, otherwise a threshold value equal to σ_B is considered. In cases where the concentration was below the method detection limit (MDL), or not detectable above the average variability of the field blanks, a concentration value equal to the maximum between the MDL and σ_B was assumed. The MDL for a specific element is calculated transforming in concentration the LOD of the analytical methodology used for chemical analysis. This represents the minimum concentration of the specific element detectable by the analytical methodology used. The approach followed is the same already applied in several source apportionment studies [19–21].

3. Results and Discussion

3.1. PM_{10} and $PM_{2.5}$ Concentrations

A summary of measured PM_{10} and $PM_{2.5}$ concentrations is reported in Table 1. Table 1 includes the numbers of available data, the percentages of rainy days (*i.e.*, days with precipitations ≥ 0.4 mm), the average concentrations, the standard deviations, the minimum and maximum values of PM_{10} and $PM_{2.5}$, and the ratio $R = PM_{2.5}/PM_{10}$ for the different sites analyzed. The statistics were also evaluated grouping together the sites with the same characteristics (background, industrial, and urban). Finally,

the last row values refer to the whole area studied (average over all measurements). The average R (0.65 ± 0.11) is in agreement with the typical European average: 0.66 [22]. In Putaud *et al.* [8] a range for R is reported in different European sites between 0.44 and 0.90 with a tendency to smaller values at low PM_{10} concentrations in rural and background sites. The average value of R for the industrial sites (0.67 ± 0.10) is the same of the urban site (0.67 ± 0.12), while, the average R calculated for background sites is significantly lower (0.61 ± 0.10), according to the t-Student test at 5% probability. This could be explained as due to the larger anthropogenic emissions of fine particles (sub-micrometric range) of urban and industrial releases. Table 1 indicates that that both $PM_{2.5}$ and PM_{10} show an increase moving from background sites to industrial and to urban sites. The concentration levels and the trend observed are in agreement with the results obtained in other European areas [23,24]. These increases are statistically significant, with the exclusion of the difference between industrial and urban in $PM_{2.5}$, at 5% probability according to the t-Student test.

During the different measurements, 51 excesses of the threshold of PM_{10} daily concentration (50 $\mu g/m^3$ fixed in European Air Quality Standards, AQS) were observed (Table 2). This corresponds to 10.6% of the measured days as an average over the studied area. However, the occurrence of the excesses of AQS threshold is significantly lower in background sites typology (4.9%) with respect to industrial typology (12.9%) and urban typology (21.5%). The EU-Directive 2008/50/CE has not established a daily threshold for $PM_{2.5}$ concentration but only a yearly limit fixed at 1/2 of that relative to PM_{10}. However, given that most of the influence of SD is on short-term (daily) concentrations, it is useful to investigate the strength of the effect on daily $PM_{2.5}$ concentrations. For this reason it has been hypothesized an indicative daily threshold of 25 $\mu g/m^3$ for $PM_{2.5}$ for the analysis of the present data.

The statistics of the excesses of this hypothesized threshold is also reported in Table 2. The behavior is similar to that observed in PM_{10} with lower occurrence of excesses of the threshold in background sites. This means that local pollution sources have an important role in determining the overcome of AQS in terms of daily concentration peaks in urban and industrial sites. The excesses observed in background sites are likely associated with long-range transport of pollution.

For each measurement day the advection of African Dust (in the following SD cases) has been investigated, considering the concentration of typical crustal elements (Fe, Al, Ti), the dust transport predictions of the DREAM model [25], the five-day back-trajectories calculated with HYSPLIT [26], and the satellite images (MODIS).

A day has been classified as a SD case if there was evidence of a dust advection from DREAM model and/or satellite images concomitant with a transport from the Sahara-Sahel area observed with back-trajectories. These events had different strength and, in general terms, were visible as an increase in daily concentrations of crustal elements. In some periods additional measurements such as LIDAR dust load vertical profiles and PM_{10} data from the fixed monitoring network were available and used for identification of SD events that generally provoke an increase of PM_{10} concentration over a large spatial area and an increase of dust load at high elevation above the ground. The statistics of SD events and its association with the excesses of AQS-threshold is reported in Table 2. Referring to PM_{10} measurements, 59 SD cases, corresponding to 12.2% of measurement days, were observed. Fourteen of these cases were concomitant with excesses of the AQS threshold (corresponding to 27.5% of the excesses) as an average over the studied area. When considering the different typologies of sites, the percentages become: 66.7% for background, 22.2% for industrial and 9.5% for urban.

Table 1. Average concentrations, standard deviations, ratios $PM_{2.5}/PM_{10}$, number of samples, and precipitations for PM_{10} and $PM_{2.5}$ at the different sites (and also grouped by typology of sites) in the period 2003–2010. The last row is the combination of all data. (U = urban site; B = background site; I = industrial site).

Site		PM_{10}				$PM_{2.5}$				$PM_{2.5}/PM_{10}$	
		n°	Rain (%)	Conc. (µg/m^3)	Dev.st. (µg/m^3)	n°	Rain (%)	Conc. (µg/m^3)	Dev.st. (µg/m^3)	R	Dev.st.
Lecce	B	173	28.3	25.9 (5.9–74.6)	12.9	24	25.0	16.8 (6.0–29.4)	6.4	0.62	0.13
Seclì	B	14	21.4	27.8 (17.3–32.8)	5.0	8	12.5	21.0 (12.4–28.1)	5.4	0.74	0.08
Galatone	B	16	18.8	26.2 (12.3–57.4)	11.6	4	0.0	13.4 (10.5–19.3)	4.0	0.45	0.11
Trepuzzi	B	15	33.3	30.1 (12.8–56.2)	12.5	7	57.1	20.4 (13.0–43.9)	11.4	0.64	0.10
Leverano	B	18	16.7	26.8 (14.1–45.8)	8.2	8	25.0	16.2 (10.7–22.4)	3.8	0.62	0.09
Nardò	B	10	40.0	24.9 (14.4–78.9)	19.4	/	/	/	/	/	/
Maglie	I	80	37.5	29.9 (5.6–100.3)	17.3	35	45.7	23.1 (8.1–66.3)	12.9	0.75	0.15
Collemeto	I	19	15.8	38.2 (18.9–52.3)	8.8	7	14.3	21.4 (15.1–31.9)	5.4	0.55	0.07
Cutrofiano	I	40	27.5	35.6 (15.3–77.2)	15.0	14	28.6	27.8 (16.3–43.4)	10.6	0.71	0.09
Lecce	U	33	18.2	27.8 (12.0–58.1)	8.4	13	23.0	14.9 (8.2–22.7)	4.3	0.54	0.13
Tricase	U	10	30.0	57.7 (22.0–127.8)	32.2	5	40.0	40.1 (19.8–92.3)	30.1	0.64	0.06
Copertino	U	14	57.1	41.5 (19.5–69.5)	15.7	5	40.0	36.2 (14.7–61.7)	16.7	0.77	0.12
Nardò	U	15	13.3	49.9 (24.3–90.6)	19.3	7	0.0	36.8 (20.6–71.0)	17.3	0.66	0.10
Maglie	U	12	25.0	41.9 (24.3–75.4)	15.8	10	20.0	32.7 (13.4–67.0)	17.3	0.72	0.12
Lequile	U	14	42.8	31.9 (17.8–64.2)	11.8	7	42.8	24.9 (11.3–55.2)	14.9	0.66	0.16
Total Background	B	246	27.2	26.3 (5.9–78.9)	12.4	51	25.5	17.6 (6.0–43.9)	6.8	0.61	0.10
Total Industrial	I	139	31.6	32.7 (5.6–100.3)	16.0	56	37.5	24.1 (8.1–66.3)	11.7	0.67	0.10
Total Urban	U	98	28.6	38.5 (12.0–127.8)	18.9	47	25.0	28.4 (8.2–92.3)	18.0	0.67	0.12
Studied Area	/	483	28.8	34.4 (5.6–127.8)	14.3	154	29.9	24.7 (6.0–92.3)	11.5	0.65	0.11

Table 2. Analysis of the excesses of the daily concentration thresholds, of the cases of advection of Saharan Dust (SD) and their connection with observed excesses. The analysis is reported for the different typologies of sites and for the studied area considering all the sites together (studied area, last row).

Typology of Site			**PM_{10}**		
	n° samples	Samples > 50 μg/m^3	Samples with SD	Samples > 50 μg/m^3 with SD	% of excesses associated with SD
Background	246	12 (4.9%)	41 (16.7%)	8	66.7
Industrial	139	18 (12.9%)	13 (8.6%)	4	22.2
Urban	98	21 (21.5%)	5 (5.1%)	2	9.5
Studied Area	483	51 (10.6%)	59 (12.2%)	14	27.5
Typology of Site			**$PM_{2.5}$**		
	n° samples	Samples > 25 μg/m^3	Samples with SD	Samples > 25 μg/m^3 with SD	% of excesses associated with SD
Background	51	6 (11.8%)	10 (19.6%)	2	33.3
Industrial	56	19 (33.9%)	3 (5.4%)	2	10.5
Urban	47	21 (44.7%)	3 (6.4%)	3	14.3
Studied Area	154	46 (29.9%)	16 (10.4%)	7	15.2

This indicates that the advections of Saharan dust have an important role in determining a relevant part of the excesses of AQS threshold observed, especially in background sites in the area. The influence of SD events on industrial and urban sites is lower due to the importance of local sources with respect to long-range transport. In Table 2 similar analysis is reported for $PM_{2.5}$. The percentages of the excesses of the hypothesized threshold associated with SD events were lower: 33.3% for background, 10.5% for industrial and 14.3% for urban. The results indicate that the background sites were more influenced than industrial/urban sites. The reduced effects of SD cases on $PM_{2.5}$, with respect to PM_{10}, can be explained considering that the SD contribution is mainly characterized by coarse particles and a significant decrease of the $PM_{2.5}/PM_{10}$ ratio is generally observed during these events [27]. However, there is evidence that SD events in the area studied are characterized by aerosol with a number distribution peaked at about 2 μm being thereby able to influence $PM_{2.5}$ [28].

An analysis of measured concentrations has been performed separating the hot weather (April to September) from cold weather (October to March). The results are reported in Tables 3 and 4. For $PM_{2.5}$, only the average values over the studied area are reported due to the limited number of samples (with respect to PM_{10}), which did not allow the distinctions between the different typologies of site. Even if with some limitations due to the different number of samples available in hot and cold weather, the inter-comparison of results for PM_{10} indicate that urban sites present a statistically significant increase of the average concentration during the cold weather that is likely associated with the anthropogenic emissions of traffic and domestic heating. Instead, the background sites show a decrease of the average concentration during the cold weather.

This could be due to the large frequency of advections of Saharan dust observed in the spring and summer periods (Table 3). This is observed in all typology of sites, but, as already mentioned it has a larger effect on background sites. The seasonal difference on the average concentration for industrial sites is not statistically significant. Considering the average over the studied area, the PM_{10} concentrations

in the hot and cold weather are essentially the same (no statistical significant difference), instead, $PM_{2.5}$ concentrations show a significant increase in the cold season. The different behavior of PM_{10} and $PM_{2.5}$ could be explained considering that the SD events have a lower importance on $PM_{2.5}$ because the dust is mainly in the coarse size-range. Thereby, the increase in the hot weather of this contribution is not able to compensate the decrease of anthropogenic emissions (traffic and domestic heating) in $PM_{2.5}$ concentrations as it does in PM_{10} concentrations. The larger importance of SD events in the hot weather is in agreement with other observations reported in literature [19,28].

Table 3. Analysis of seasonal trends of concentrations, of excesses of the daily concentration threshold, of the cases of advection of Saharan Dust (SD) and their connection with observed excesses for $PM_{2.5}$ and PM_{10} as an average over the studied area.

	$PM_{2.5}$		**PM_{10}**	
	Studied Area		**Studied Area**	
	Hot Season	**Cold Season**	**Hot Season**	**Cold Season**
n° samples	60	94	193	290
Concentration (μg/m^3)	19.1 (6.0–66.3)	25.8 (7.6–92.3)	29.1 (5.6–80.0)	31.6 (7.0–127.8)
St. Dev.	10.3	14.5	13.7	16.9
SD events (occurrence)	9 (15.0%)	7 (7.4%)	38 (19.7%)	21 (7.2%)
Samples > 50 μg/m^3 (occurrence)	/	/	13 (6.7%)	38 (13.1%)
Samples > 25 μg/m^3 (occurrence)	12 (20.0%)	34 (56.7%)	/	/
Samples > 50 μg/m^3 with SD	/	/	10	4
Samples > 25 μg/m^3 with SD	4	3	/	/
% of excesses associated with SD	33.3	8.8	76.9	10.5

Table 4. Analysis of seasonal trends of concentrations, of excesses of the daily concentration threshold, of the cases of advection of Saharan Dust (SD) and their connection with observed excesses for PM_{10} considering the different typologies of sites.

	PM_{10}					
	Background		**Industrial**		**Urban**	
	Hot Season	**Cold Season**	**Hot Season**	**Cold Season**	**Hot Season**	**Cold Season**
n° samples	141	105	37	102	15	83
Concentration (μg/m^3)	28.1 (5.9–80.0)	23.9 (7.0–78.9)	33.7 (5.6–78.4)	32.3 (9.00–100.3)	27.2 (12.0–48.8)	40.5 (16.8–127.8)
St. Dev.	12.4	12.2	19.0	14.9	7.3	19.7
SD events (occurrence)	30 (21.3%)	11 (10.5%)	8 (21.6%)	5 (4.9%)	0 (0%)	5 (6.0%)
Samples > 50 μg/m^3 (occurrence)	7 (4.9%)	5 (4.7%)	6 (16.2%)	12 (11.7%)	0 (0%)	21 (25.3%)
Samples > 25 μg/m^3 (occurrence)	/	/	/	/	/	/
Samples > 50 μg/m^3 with SD	6	2	4	0	0	2
Samples > 25 μg/m^3 with SD	/	/	/	/	/	/
% of excesses associated with SD	85.7	40.0	66.7	0.0	0.0	9.5

Long-terms datasets of atmospheric concentrations are often described with lognormal distributions [18,29,30]. This is confirmed by the chi-square test, applied to our PM_{10} and $PM_{2.5}$ time series. Lognormal distribution fits have been used to evaluate the effect of the SD events on long-term concentrations and excesses of the daily thresholds. A fit with a lognormal distribution has been performed for the total dataset and for a dataset in which the SD events were removed. Results for the different typologies of sites and for the studied area are presented in Table 5. Results in Table 5 indicate that SD events have a limited effect on long-term average concentrations (3.4% increase of average PM_{10} and 1.5% increase of average $PM_{2.5}$). This is in agreement with the observations made in Spain [24]. There is an increase in the probability of overcome of the daily concentration threshold fixed in AQS for PM_{10} and hypothesized in this work for $PM_{2.5}$. This is particularly evident for PM_{10} in background sites, in which this probability is more than doubled.

Table 5. Results of the fit with lognormal distributions in terms of average concentrations and probabilities to overcome the daily thresholds (fixed in AQS for PM_{10} and hypothesized in this work for $PM_{2.5}$). Results are reported for the total dataset and also excluding the SD cases.

	Type Sites		**Average (µg/m^3)**	**Probability (%) [PM_{10}] > 50 µg/m^3**	**Probability (%) [$PM_{2.5}$] > 25 µg/m^3**
PM_{10}	Background	Total	23.7	5.2	/
		No SD	22.4	2.4	/
	Industrial	Total	29.3	13.3	/
		No SD	28.5	11.7	/
	Urban	Total	35.0	19.9	/
		No SD	34.4	18.7	/
	Studied Area	Total	27.3	10.4	/
		No SD	26.4	8.5	/
$PM_{2.5}$	Background	Total	16.4	/	13.6
		No SD	16.1	/	13.3
	Industrial	Total	21.7	/	37.8
		No SD	21.2	/	35.8
	Urban	Total	24.1	/	47.3
		No SD	23.2	/	44.9
	Studied Area	Total	20.4	/	34.1
		No SD	20.1	/	33.1

3.2. Metal Content in PM_{10} and $PM_{2.5}$

At all sites, metals concentrations in PM_{10} and in $PM_{2.5}$ were determined in order to investigate the possible sources and the PM formation mechanisms [31]. The concentrations and their variability are reported in Table 6 (for PM_{10}) and in Table 7 (for $PM_{2.5}$). The concentrations are reported in absolute values (ng/m^3) and in relative values (µg/g) and the sites are grouped by typology. In cases where the concentration of a specific metal was not quantified for more than 50% of the samples an average concentration was not reported and a threshold value was indicated in Table 7. As and Sb levels were commonly not quantified in PM_{10} and difficulties were also encountered for Cd in the $PM_{2.5}$ fraction.

In average terms the trace metals analyzed represent 2.0% of PM_{10} (average over the studied area) and 0.86% of $PM_{2.5}$.

Table 6. Absolute and relative concentrations of metals contained in PM_{10} for the different typologies of sites and as average for the studied area. In parenthesis the observed ranges.

PM_{10}		Background (Samples 185)	Industrial (Samples 137)	Urban (Samples 97)	Studied Area (Samples 419)
Cd	ng/m^3	**0.2** (0.01–0.8)	**0.3** (0.01–1.0)	**<0.6**	**0.3** (0.01–7.7)
	µg/g	**5.9** (0.2–53.8)	**8.1** (0.4–47.5)	**<16.2**	**9.6** (0.2–344.5)
V	ng/m^3	**1.5** (0.1–6.3)	**1.8** (0.1–12.3)	**<1.9**	**1.7** (0.1–12.3)
	µg/g	**58.6** (1.8–280.0)	**58.8** (3.7–344.4)	**<55.8**	**57.8** (1.4–344.4)
Fe	ng/m^3	**270.0** (7.8–2241.9)	**227.1** (10.9–1750.8)	**229.2** (21.4–649.4)	**246.7** (7.8–2241.9)
	µg/g	**9362.2** (271.9–34135.0)	**7052.2** (267.2–58600.1)	**6474.1** (428.7–20561.6)	**7956.0** (267.2–58600.1)
Al	ng/m^3	**293.9** (9.1–3993.6)	**115.7** (3.5–521.1)	**391.1** (40.4–507.7)	**269.7** (3.5–3993.6)
	µg/g	**9952.4** (669.9–51115.6)	**4236.6** (135.2–22851.3)	**14948.4** (949.7–29758.3)	**9502.2** (135.2–51115.6)
Cu	ng/m^3	**9.9** (0.4–114.2)	**8.5** (0.5–80.6)	**11.9** (1.0–40.9)	**9.8** (0.4–114.2)
	µg/g	**373.9** (19.1–2967.4)	**280.4** (12.4–4114.0)	**312.7** (33.4–1567.3)	**330.0** (12.4–4114.0)
Ni	ng/m^3	**2.7** (0.2–46.7)	**5.2** (0.1–174.0)	**2.2** (0.3–17.8)	**3.5** (0.1–174.0)
	µg/g	**107.9** (9.5–1674.7)	**152.6** (3.5–5822.9)	**62.2** (4.8–451.1)	**116.0** (3.5–5822.9)
Mn	ng/m^3	**6.8** (0.2–59.5)	**3.6** (0.04–32.6)	**4.2** (0.2–11.7)	**5.2** (0.04–59.5)
	µg/g	**246.5** (7.0–1011.7)	**113.4** (1.5–1091.2)	**114.5** (1.4–297.8)	**176.0** (1.4–1091.2)
Zn	ng/m^3	**21.8** (2.2–215.2)	**33.6** (1.0–280.4)	**23.2** (2.4–78.0)	**26.0** (1.0–280.4)
	µg/g	**930.4** (60.2–15072.6)	**1293.0** (31.2–17307.1)	**630.7** (118.6–2705.2)	**981.5** (31.3–17307.1)
Pb	ng/m^3	**7.3** (0.4–106.3)	**11.9** (0.7–92.4)	**10.0** (0.7–77.9)	**8.9** (0.4–106.3)
	µg/g	**273.9** (25.5–2775.3)	**434.4** (29.7–5008.8)	**257.8** (15.9–2633.7)	**314.1** (15.9–5008.8)
As	ng/m^3	**<0.9**	**<0.9**	**<0.8**	**<0.9**
	µg/g	**<41.8**	**<40.6**	**<22.7**	**<38.1**

Table 6. *Cont.*

PM_{10}		Background (Samples 185)	Industrial (Samples 137)	Urban (Samples 97)	Studied Area (Samples 419)
Cr	ng/m^3	**2.5** (0.1–41.7)	**13.5** (0.1–406.7)	**2.5** (0.3–35.7)	**5.3** (0.1–406.7)
	µg/g	**91.3** (6.8–1083.7)	**371.9** (5.7–13612.7)	**67.5** (5.4–906.0)	**157.3** (5.4–13612.7)
Sb	ng/m^3	**<2.3**	**<1.2**	**<2.5**	**<2.1**
	µg/g	**<95.3**	**<50.8**	**<89.8**	**<86.0**
Ti	ng/m^3	**15.2** (0.1–229.7)	**5.5** (0.9–16.2)	**8.2** (0.3–96.3)	**11.3** (0.4–229.7)
	µg/g	**499.8** (8.4–2911.8)	**232.9** (14.1–871.9)	**265.9** (10.9–2821.2)	**384.7** (8.4–2911.8)

Table 7. Absolute and relative concentrations of metals contained in $PM_{2.5}$ for the different typologies of sites and as average for the studied area. In parenthesis the observed ranges.

$PM_{2.5}$		Background (Samples 32)	Industrial (Samples 52)	Urban (Samples 29)	Studied Area (Samples 113)
Cd	ng/m^3	**<0.4**	**<0.2**	**<0.4**	**<0.3**
	µg/g	**<14.6**	**<11.4**	**<13.7**	**<12.9**
V	ng/m^3	**<1.4**	**1.5** (0.1–5.0)	**<1.7**	**1.5** (0.1–5.0)
	µg/g	**<90.5**	**62.7** (4.6-192.5)	**<65.5**	**75.5** (2.0–714.3)
Fe	ng/m^3	**86.8** (0.9–416.9)	**85.0** (10.9–333.8)	**78.8** (3.9–346.9)	**83.9** (0.9–416.9)
	µg/g	**4621.4** (51.6–15285.7)	**3141.4** (666.7–10570.8)	**3004.2** (148.3–14304.3)	**3515.5** (51.6–15285.7)
Al	ng/m^3	**60.7** (15.0–144.9)	**66.7** (1.7–206.9)	**51.0** (4.5–157.3)	**62.7** (1.7–206.9)
	µg/g	**3654.7** (341.3–7050.0)	**2291.4** (87.0–6742.2)	**2211.3** (167.9–6487.7)	**2677.3** (1.7–206.9)
Cu	ng/m^3	**3.1** (0.1–22.1)	**5.1** (0.9–31.3)	**5.7** (1.0–15.6)	**4.7** (0.1–31.3)
	µg/g	**158.3** (6.8–1511.5)	**231.6** (19.4–1688.1)	**217.1** (44.4–616.3)	**207.1** (6.8–1688.1)
Ni	ng/m^3	**2.4** (0.3–30.4)	**1.9** (0.2–13.7)	**1.7** (0.4–3.4)	**2.0** (0.2–30.4)
	µg/g	**150.0** (12.5–1628.1)	**73.8** (5.8–315.4)	**57.2** (13.3–143.2)	**90.9** (5.8–1628.1)
Mn	ng/m^3	**2.3** (0.2–4.5)	**1.7** (0.01–8.4)	**1.9** (0.2–5.4)	**1.9** (0.01–8.4)
	µg/g	**117.7** (12.5–207.1)	**63.1** (0.7–265.6)	**63.0** (2.0–166.6)	**78.3** (0.7–265.6)

Table 7. *Cont.*

$PM_{2.5}$		Background (Samples 32)	Industrial (Samples 52)	Urban (Samples 29)	Studied Area (Samples 113)
Zn	ng/m^3	**14.9** (2.4–76.4)	**30.8** (2.0–154.1)	**25.7** (7.3–131.6)	**24.7** (2.1–154.1)
	µg/g	**1004.0** (90.9–7476.2)	**1527.9** (38.0–10615.0)	**896.3** (214.4–4750.2)	**1205.9** (38.0–10615.0)
Pb	ng/m^3	**9.5** (0.7–65.7)	**8.6** (1.3–39.8)	**8.5** (0.7–31.1)	**8.9** (0.7–65.7)
	µg/g	**472.1** (29.1–4478.4)	**365.6** (24.1–2207.6)	**260.7** (44.0–1157.5)	**369.7** (24.1–4478.4)
As	ng/m^3	**1.0** (0.9–3.1)	**0.7** (0.01–1.0)	**<0.8**	**0.8** (0.01–3.1)
	µg/g	**76.8** (14.6–714.3)	**34.6** (0.4–113.5)	**<31.0**	**46.1** (0.2–714.3)
Cr	ng/m^3	**1.9** (0.5–13.5)	**3.0** (0.1–13.3)	**1.4** (0.1–3.7)	**2.2** (0.1–13.5)
	µg/g	**106.8** (8.4–921.8)	**102.7** (6.1–321.4)	**58.0** (2.9–139.7)	**90.9** (2.3–921.8)
Sb	ng/m^3	**1.6** (0.9–6.8)	**1.2** (0.4–3.0)	**1.0** (0.9–1.5)	**1.2** (0.4–6.8)
	µg/g	**99.1** (20.8–497.9)	**53.3** (9.9–218.7)	**49.6** (16.3–80.2)	**66.1** (9.8–497.9)
Ti	ng/m^3	**4.9** (0.9–12.3)	**2.7** (0.9–6.4)	**0.9** (0.09–0.9)	**3.1** (0.09–12.3)
	µg/g	**299.8** (20.8–737.2)	**105.4** (41.1–262.4)	**46.8** (16.3–80.2)	**159.1** (16.3–737.2)

Table 8. Correlation matrix for PM_{10} concentrations evaluated for the studied area. In bold values larger than 0.65.

PM_{10}	Fe	V	Ni	Cd	Cu	Zn	Mn	Pb	Cr	Al	Ti
Fe	1.00	0.30	0.42	0.03	0.33	0.06	**0.83**	0.17	0.45	**0.82**	**0.72**
V		1.00	0.10	0.09	0.09	0.04	0.27	0.06	0.09	0.27	0.24
Ni			1.00	0.04	0.08	0.14	0.40	0.20	**0.96**	0.08	0.07
Cd				1.00	0.17	0.10	0.05	0.11	0.02	−0.22	−0.25
Cu					1.00	0.27	0.29	0.36	0.07	0.06	−0.01
Zn						1.00	0.03	0.40	0.21	0.03	−0.05
Mn							1.00	0.13	0.36	**0.82**	**0.68**
Pb								1.00	0.21	−0.03	−0.06
Cr									1.00	0.19	0.31
Al										1.00	**0.79**
Ti											1.00

There is not a clear pattern in metals concentrations in $PM_{2.5}$ comparing the three typologies of sites. However, in PM_{10} significantly larger concentrations of Cd, Pb, and Cr are observed in industrial

sites with respect to background sites (according to the t-Student test at 5% probability); while crustal elements (Al, Mn, and Ti) have larger concentrations in background sites.

The comparison of metal concentrations in different typologies of sites has been performed, for example, in Spain [23,24] and in other locations in Central and Northern Europe [32,33]. However, detailed results for the area investigated are not available. In general terms, trace element concentrations do not show clear trends moving from one typology of site to the other. In [32], two groups of metals have been identified one increasing in urban sites and the other being substantially similar at all typology of sites.

Figure 2. Crustal enrichment factors calculated for PM_{10} and $PM_{2.5}$ in the different typologies of sites including the average for the studied area.

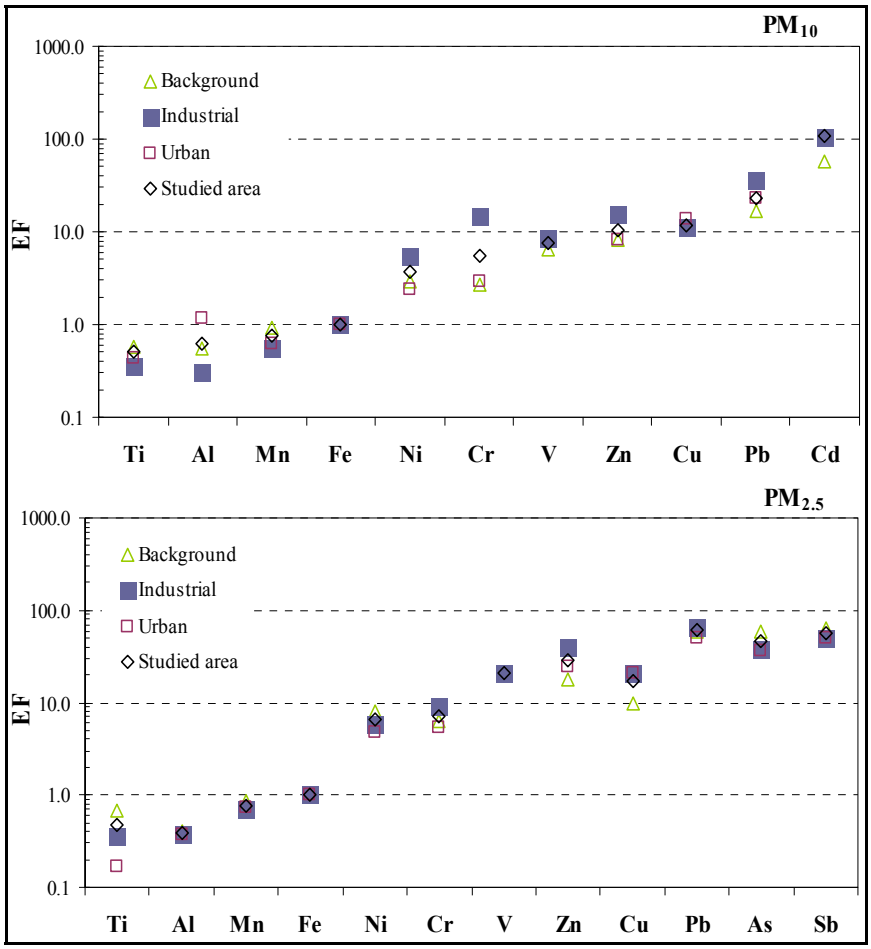

The crustal enrichment factors (EFs) were evaluated for the different elements in PM_{10} and $PM_{2.5}$ fractions taking Fe as reference element and using, for comparison, the average re-suspended soil composition determined in the area studied [34]. The EFs are reported in Figure 2. Calculations were not performed for cases in which only a threshold value is given in Tables 6 and 7 (*i.e.*, when more than 50% of the samples were not quantified). Fe is not the only possible choice for crustal reference, but it is one commonly used in calculation of EFs [35–41]. The analysis of EFs furnishes only qualitative information, because the wide variation of the elemental concentration must also be considered. Here the two-threshold system developed by Cesari *et al.* [34] is used. EF larger than 4 can be considered mainly of anthropogenic origin (elements significantly enriched), while elements with

EF smaller than 2 can be considered mainly of crustal origin. Between the two thresholds elements are likely influenced by both crustal and anthropogenic sources. The elements Ti, Al, and Mn are not enriched in both fractions (PM_{10} and $PM_{2.5}$) for all typologies of sites. Ni and Cr appear to be enriched in $PM_{2.5}$ and in PM_{10} for industrial sites but a significant crustal component could be present at background and urban sites for these elements in PM10. V, Cu, Pb, Zn, Cd, and Sb are significantly enriched at all typologies of sites; particularly, in literature, many of these highly enriched metals have been associated with traffic source [42]. In general, the enrichment of a specific element is larger in the $PM_{2.5}$ fraction [43]. In Table 8, the correlation matrix for the metals in PM_{10} calculated over all the studied area is presented. It is observed a correlation between the low-enrichment elements Fe, Al, Mn, and Ti, likely of crustal origin [34]. A second correlation between Ni and Cr is observed, especially in industrial sites. This correlation is commonly associated with industrial emissions like pyrometallurgical processes such as those in steel plants and in non-ferrous metal industries [42,43]. In urban sites (not shown) a correlation between Cu and Sb is observed likely associated with the traffic contribution. These elements showed significant increase at traffic spot in Barcelona likely due to break abrasion [24]. The correlation matrix for $PM_{2.5}$ (not shown) gave the same groups of elements correlated.

4. Conclusions

The analysis reported shows that PM_{10} and $PM_{2.5}$ concentrations in the Salentum peninsula are increasing moving from background sites to industrial and to urban sites. However, the $PM_{2.5}/PM_{10}$ ratio is significantly lower (0.61 ± 0.10) at background sites with respect to industrial and urban sites. Even if the samples available are limited, the t-Student test applied to this specific dataset allowed to infer that urban sites show a statistically significant increase of PM_{10} average concentrations during the cold weather, likely due to anthropogenic urban emissions. Instead, the background sites show a decrease of the average concentrations in the cold weather. This may be due to increase of the frequency of Saharan dust advection in the spring and summer periods that is observed in all typology of sites, but, it has a larger effect on concentrations at background sites. The seasonal difference on the average concentration for industrial sites is not statistically significant. The advection of SD has an influence on both PM_{10} and $PM_{2.5}$ concentrations; however the effect is significantly larger in background sites with respect to urban and industrial sites. Over the studied area, the effect is relatively limited on long-term average PM_{10} (estimated increase of 3.2%) and $PM_{2.5}$ (estimated increase of 1.5%) concentrations but it is larger on the daily concentrations. It is estimated an increase of 22% of the probability to overcome the air quality standard threshold for PM_{10}, as an average over the studied area, and of 3% regarding the hypothesized threshold for $PM_{2.5}$. However, the probabilities are more than doubled in background sites.

Metals in PM_{10} indicate an increase of Cd, Pb, and Cr in industrial sites with respect to background sites (according to the t-Student test at 5% probability). Instead crustal elements (Al, Mn, and Ti) have larger concentrations in background sites. Average concentrations of metals in $PM_{2.5}$ do not show a clear dependence on site typology. This could be a consequence of the more limited statistics available on $PM_{2.5}$. On average, Al, Mn, Fe, and Ti have a low enrichment factor being mainly of crustal origin and well-correlated one with the other. Ni and Cr are correlated and significantly enriched at industrial sites in both PM_{10} and $PM_{2.5}$. This indicates the possible presence of an industrial source of Ni and Cr.

Further, V, Cu, Pb, Zn, Cd, and Sb are significantly enriched with respect to local soil in all typologies of sites.

Acknowledgments

The financial support of the Environmental Office of the Provincial Government of Lecce, through a six years (2003–2008) collaborative Project, is gratefully acknowledged. Authors also thank the Project I-AMICA (Infrastruttura di Alta tecnologia per il Monitoraggio Integrato Climatico-Ambientale, PON a3_00363), funded under the National Operational Programme (NOP) for "Research and Competitiveness 2007–2013", co-funded with European Regional Development Fund (ERDF) and National resource. Authors wish to thank S. Francioso of the Provincial Government of Lecce and F. M. Grasso of the Lecce Section of ISAC-CNR.

Author Contributions

The work has been performed in collaboration between all the authors. Daniele Contini and Franco Belosi coordinated the activities and collaborated at the measurements and interpretation of results. Antonio Donateo and Daniela Cesari collaborated at the experiments and at part of the data processing and interpretation. Daniela Chirizzi collaborated at part of the data processing and results interpretation.

Conflicts of Interest

The authors declare no conflict of interest.

References

1. Seinfeld, J.H.; Pandis, S.N. *Atmospheric Chemistry and Physics: From Air Pollution to Climate Change*; John Wiley & Sons: New York, NY, USA, 1998.
2. Pope, C.A.; Dockery, D.W. Health effects of fine particulate air pollution: Lines that connect. *J. Air Waste Manag.* **2006**, *56*, 709–742.
3. Khan, M.F.; Hirano, K.; Masunaga, S. Quantifying the sources of hazardous elements of suspended particulate matter aerosol collected in Yokohama, Japan. *Atmos. Environ.* **2010**, *44*, 2646–2657.
4. Kim, N.K.; Kim, Y.P.; Kang, C.H. Long-term trend of aerosol composition and direct radiative forcing due to aerosols over Gosan: TSP, PM10, and PM2.5 Data between 1992 and 2008. *Atmos. Environ.* **2011**, *45*, 6107–6115.
5. Solomon, S.; Qin, D.; Manning, M.; Chen, Z.; Marquis, M.; Averyt, K.B.; Tignor, M.; Miller, H.L. *Climate Change 2007: The Physical Science Basis*; Cambridge University Press: Cambridge, UK/New York, NY, USA, 2007.
6. Barmpadimos, I.; Nufer, M.; Oderbolz, D.C.; Keller, J.; Aksoyoglu, S.; Hueglin, C.; Baltensperger, U.; Prévôt, A.S.H. The weekly cycle of ambient concentrations and traffic emissions of coarse (PM10-PM2.5) atmospheric particles. *Atmos. Environ.* **2011**, *45*, 4580–4590.
7. McBride, S.J.; Norris, G.A.; Williams, R.W.; Neas, L.M. Bayesian hierarchical modeling of cardiac response to particulate matter exposure. *J. Exp. Sci. Environ. Epidemiol.* **2011**, *21*, 74–91.

8. Putaud, J.P.; Van Dingenen, R.; Alastuey, A.; Bauer, H.; Birmili, W.; Cyrys, J.; Flentje, H.; Fuzzi, S.; Gehrig, R.; Hansson, H.C. European aerosol phenomenology–3: Physical and chemical characteristics of particulate matter from 60 rural, urban and kerbside sites across Europe. *Atmos. Environ.* **2010**, *44*, 1308–1320.
9. Mallone, S.; Strafoggia, M.; Faustini, A.; Gobbi, G.P.; Marconi, A.; Forastiere, F. Saharan dust and associations between particulate matter and daily mortality in Rome, Italy. *Environ. Health Perspect.* **2011**, *119*, 1409–1414.
10. Reyes, M.; Díaz, J.; Tobias, A.; Montero, J.C.; Linares, C. Impact of Saharan dust particles on hospital admissions in Madrid (Spain). *Int. J. Environ. Health Res.* **2014**, *24*, 63–72.
11. Karanasiou, A.; Moreno, N.; Moreno, T.; Viana, M.; de Leeuw, F.; Querol, X. Health effects from Sahara dust episodes in Europe: Literature review and research gaps. *Environ. Int.* **2012**, *47*, 107–114.
12. Escudero, M.; Querol, X.; Pey, J.; Alastuey, A.; Pérez, N.; Ferreira, F.; Alonso, S.; Rodriguez, S.; Cuevas, E. A methodology for the quantification of the net African dust load in air quality monitoring networks. *Atmos. Environ.* **2007**, *41*, 5516–5524.
13. Querol, X.; Pey, J.; Pandolfi, M.; Alastuey, A.; Cusack, M.; Pérez, N.; Moreno, T.; Viana, M.; Mihalopoulos, N.; Kallos, G.; *et al.* African dust contributions to mean ambient PM10 mass-levels across the Mediterranean Basin. *Atmos. Environ.* **2009**, *43*, 4266–4277.
14. Viana, M.; Pey, J.; Querol, X.; Alastuey, A.; de Leeuw, F.; Lukewille, A. Natural sources of atmospheric aerosols influencing air qualità across Europe. *Sci. Total Environ.* **2014**, *472*, 825–833.
15. Rodriguez, S.; Querol, X.; Alastuey, A.; Mantilla, E. Origin of high summer PM10 and TSP concentrations at rural sites in Eastern Spain. *Atmos. Environ.* **2002**, *36*, 3101–3112.
16. Pateraki, S.T.; Assimakopoulos, V.D.; Maggos, T.H.; Famelia, K.M.; Kotroni, V.; Vasilakos, C.H. Particulate matter pollution over a Mediterranean urban area. *Sci. Total Environ.* **2013**, *463*, 508–524.
17. Paik, S.; Vincent, J.H. Filter and cassette mass instability in ascertaining the limit of detection of inhalable airborne particulates. *AIHA J.* **2002**, *63*, 698–702.
18. Belosi, F.; Contini, D.; Donateo, A.; Prodi, F. Measurements of atmospheric aerosol in the Salentum Penisola and its correlation with local meteorology. *Il Nuovo Cimento* **2006**, *29*, 473–486.
19. Contini, D.; Genga, A.; Cesari, D.; Siciliano, M.; Donateo, A.; Bove, M.C.; Guascito, M.R. Characterization and source apportionment of PM10 in an urban background site in Lecce. *Atmos. Res.* **2010**, *95*, 40–54.
20. Contini, D.; Donateo, A.; Cesari, D.; Belosi, F.; Francioso, S. Identification and characterisation of local aerosol sources using high temporal resolution measurements. *J. Environ. Monit.* **2010**, *12*, 1709–1721.
21. Contini, D.; Cesari, D.; Genga, A.; Siciliano, M.; Ielpo, P.; Guascito, M.R.; Conte, M. Source apportionment of size-segregated atmospheric particles based on the major water-soluble components in Lecce (Italy). *Sci. Total Environ.* **2014**, *472*, 248–261.
22. CAFE Working Group on Particulate Matter. Second Position Paper on Particulate Matter. European Working Group on Particulate Matter. Available online: http://ec.europa.eu/environment/archives/cafe/pdf/working_groups/2nd_position_paper_pm.pdf (accessed on 21 May 2014)
23. Querol, X.; Alastuey, A.; Ruiz, C.R.; Artiñano, B.; Hansson, H.C.; Harrison, R.M.; Buringh, E.; ten Brink, H.M.; Lutz, M.; Bruckmann, P.; *et al.* Speciation and origin of PM10 and PM2.5 in selected European cities. *Atmos. Environ.* **2004**, *38*, 6547–6555.

24. Querol, X.; Alastuey, A.; Moreno, T.; Viana, M.M.; Castillo, S.; Pey, J.; Rodríguez, S.; Artiñano, B.; Salvador, P.; Sánchez, M.; *et al.* Spatial and temporal variations in airborne particulate matter (PM10 and PM2.5) across Spain 1999–2005. *Atmos. Environ.* **2008**, *42*, 3964–3979.
25. Centro National de Supercomputaciòn, Barcelona Supercomputing Center. DREAM. Available online: http://www.bsc.es (accessed on 21 May 2014).
26. ARL Air Resources Laboratory–READY–Real-time Environmental Applications and Display sYstem. Available online: http://www.arl.noaa.gov/ready/ (accessed on 21 May 2014).
27. Querol, X.; Alastuey, A.; Rodriguez, S.; Plana, F.; Ruiz, C.R.; Cots, N.; Massagué, G.; Puig, O. PM10 and PM2.5 source apportionment in the Barcelona metropolitan area, Catalonia, Spain. *Atmos. Environ.* **2001**, *35*, 6407–6419.
28. Blanco, A.; de Tomasi, F.; Filippo, E.; Manno, D.; Perrone, M.R.; Serra, A.; Tafuro, A.M.; Tepore, A. Characterization of African dust over southern Italy. *Atmos. Chem. Phys.* **2003**, *3*, 2147–2159.
29. Kao, A.S.; Friedlander, S.K. Frequency distributions of PM10 chemical components and their sources. *Environ. Sci. Technol.* **1995**, *29*, 19–28.
30. Hadley, A.; Toumi, R. Assessing changes to the probability distribution of sulphur dioxide in the UK using a lognormal model. *Atmos. Environ.* **2003**, *37*, 1461–1474.
31. Ragosta, M.; Caggiano, R.; Macchiato, M.; Sabia, S.; Trippetta, S. Trace elements in daily collected aerosol: Level characterization and source identification in a four-year study. *Atmos. Res.* **2008**, *89*, 206–217.
32. Hueglin, C.; Gehrig, R.; Baltensperger, U.; Gysel, M.; Monn, C.; Vonmont, H. Chemical characterisation of PM2.5, PM10 and coarse particles at urban, near-city and rural sites in Switzerland. *Atmos. Environ.* **2005**, *39*, 637–651.
33. Putaud, J.P.; Raes, F.; van Dingenen, R.; Brüggemann, E.; Facchini, M.C.; Decesari, S.; Fuzzi, S.; Gehrig, R.; Hüglin, C.; Laj, P.; *et al.* A European aerosol phenomenology—2: Chemical characteristics of particulate matter at kerbside, urban, rural and background sites in Europe. *Atmos. Environ.* **2004**, *38*, 2579–2595.
34. Cesari, D.; Contini, D.; Genga, A.; Siciliano, M.; Elefante, C.; Baglivi, F.; Daniele, L. Analysis of raw soils and their re-suspended PM10 fractions: Characterisation of source profiles and enrichment factors. *Appl. Geochem.* **2012**, *27*, 1238–1246.
35. Hu, X.; Ding, Z.; Zhang, Y.; Sun, Y.; Wu, J.; Chen, Y.; Lian, H. Size distribution and source apportionment of airborne metallic elements in Nanjing, China. *Aerosol Air Qual. Res.* **2013**, *13*, 1796–1806.
36. Zhou, S.; Yuan, Q.; Li, W.; Lu, Y.; Zhang, Y.; Wang, W. Trace metals in atmospheric fine particles in one industrial urban city: Spatial variations, sources, and health implications. *J. Environ. Sci.* **2014**, *26*, 205–213.
37. Zhang, N.; Cao, J.; Xu, H.; Zhu, C. Elemental compositions of PM2.5 and TSP in Lijiang, southeastern edge of Tibetan Plateau during pre-monsoon period. *Particuology* **2013**, *11*, 63–69.
38. Cheung, K.; Daher, N.; Kam, W.; Shafer, M.M.; Ning, Z.; Schauer, J.J.; Sioutas, C. Spatial and temporal variation of chemical composition and mass closure of ambient coarse particulate matter ($PM_{10–2.5}$) in the Los Angeles area. *Atmos. Environ.* **2011**, *45*, 2651–2662.

39. Clements, N.; Eav, J.; Xie, M.; Hannigan, M.P.; Miller, S.L.; Navidi, W.; Peel, J.L.; Schauer, J.J.; Shafer, M.M.; Milford, J.B. Concentrations and source insights for trace elements in fine and coarse particulate matter. *Atmos. Environ.* **2014**, *89*, 373–381.
40. Braga, C.F.; Teixeira, E.C.; Meira, L.; Wiegand, F.; Yoneama, M.L.; Dias, J.F. Elemental composition of PM10 and PM2.5 in urban environment in South Brazil. *Atmos. Environ.* **2005**, *39*, 1801–1815.
41. Contini, D.; Belosi, F.; Gambaro, A.; Cesari, D.; Stortini, A.M.; Bove, M.C. Comparison of PM_{10} concentrations and metal content in three different sites of the Venice Lagoon: An analysis of possible aerosol sources. *J. Environ. Sci.* **2012**, *24*, 1954–1965.
42. Manno, E.; Varrica, D.; Dongarrà, G. Metal distribution in road dust samples collected in an urban area close to a petrochemical plant at Gela, Sicily. *Atmos. Environ.* **2006**, *40*, 5929–5941.
43. Xu, L.; Yu, Y.; Yu, J.; Chen, J.; Niu, Z.; Yin, L.; Zhang, F.; Liao, X.; Chen, Y. Spatial distribution and sources identification of elements in $PM_{2.5}$ among the coastal city group in the Western Taiwan Strait region, China. *Sci. Total Environ.* **2013**, *442*, 77–85.